EXPERIMENTAL STUDY OF STRENGTHENING OF RC CONTINUOUS BEAM USING FRP COMPOSITES

Chennadi Kavya Sree[1], B. Sumalatha[2] and Dr. B. Sharath Chandra[3]

[1]PG Scholar
[2]Assiatant Professor
[3]Head Of the Department

Abstract :*Strengthening projects with the recently developed Fibre Reinforced Polymer (FRP)'s outer bond strength. Because of its numerous benefits compared to traditional methods, such as high strength, low weight, resistance to corrosion, high resilience to fatigue, rapid and simple installation, and minimum change in structural geometry, In the last decade, Fiber Reinforced Polymer (FRP) composites have experienced a significant surge in popularity and adoption. In the present study, the primary objective is to investigate the performance of continuously reinforced cement concrete beams under static loading conditions using experimental methods. The beams are reinforced with Glass Fibre Reinforced Polymer (G.F.R.P.) strips externally bonded to provide additional strengthening. Various techniques have been employed in an attempt to enhance the structural capacity and behavior of the beams. The fourteen continuous (two-span) beams in this program measure 152mm*305mm*2300mm in total. The beams are divided into series and reinforced with increasing quantities of steel. With different levels of steel reinforcement in each series, the beams are divided into the S1 and S2 series. One beam of each series (S1 and S2) was left unreinforced and used as a control beam.*

The current work investigates the responses of RCC continuous beam to load deflection analysis, load capacity enhancement, and failure mechanisms. By deferring the appearance of visible fractures and decreasing fracture widths at huge load levels, the epoxy-glued layer improved the cracking performance of the continuous beams.

1. INTRODUCTION

1.1 GENERAL

Depending on the kind of construction, a structure's design life varies and is intended to last for a specified period of time. The design life of a residential building may be twenty-five years, but the design life of a public facility may be fifty years. Concrete structural deterioration is a major issue for the global infrastructure and bridge industry. Environmental conditions that can expedite or accelerate a process degradation include corrosion of steel, aging-related strength loss, repeated high-intensity loads, temperature variations, freeze-thaw cycles, contact with chemicals and

salty water, and UV radiation exposure. It will be less expensive to retrofit or reinforce the structure than to completely replace or rebuild it.

To enhance the strength and performance of existing concrete beams and columns, a common technique involves retrofitting them with externally bonded Fiber Reinforced Polymer (FRP) composites, much research is being conducted worldwide. The researchers conducted a study on retrofitted concrete beams and columns using carbon fiber reinforced polymer (CFRP/GFRP) composites. Their objective was to assess the durability, impact of confinement, provide design recommendations, and conduct experimental evaluations. They also explored strategies to enhance the ductility and strength properties of the retrofitted elements.

1.2 CURRENT RESEARCH ON FRP

Concerns about the usage of FRPs in civil applications are raised by the absence of design standards and restrictions. For over a decade, researchers from Canada, Europe, and Japan have collaborated to publish research papers aimed at providing valuable guidelines and recommendations for engineers involved in designing FRP structures.

2. LITERATURE REVIEW

F. Ceroni (2010) Under monotonic and cyclic loads—the latter of which are characterized by a low number of cycles in the elastic and post-elastic range—experiments were conducted Detailed discussions are provided on the comparisons between experimental and theoretical failure loads for Reinforced concrete (RC) beams that have been externally reinforced with carbon fiber reinforced polymer (FRP) laminates and near-surface mounted (NSM) bars.

The experimental performance of C.F.R.P strips used for flexural strengthening in the negative moment area of a full-scale reinforced concrete beam was examined by **Grace et al. in 2001.** The possibility of flexural strengthening was explored for two beam groups (I and II). For Category I and II beams, the failure mechanisms were shear and flexure, respectively. Each category's five full-scale concrete beams were evaluated. The failure of Category II beams was discovered to be caused by shear/tension delamination at the interface region where the two materials meet the C.F.R.P. strips and the concrete surface, which occurred both with and without concrete-cover failure. Localized deboning and diagonal cracking at the top of the beams caused category I beams to collapse. The C.F.R.P strips weren't fully strained when the beams dropped, resulting in ductile defects in each beam. In comparison to similar control beams, the load-carrying capacity showed the highest increase of 29% for Category I beams and 40% for Category II beams when strengthened.

But Grace et al. (2005) three continuous Experimental testing was performed on the beams in a distinct research project. Sadly, the reference beam, one of those beams, failed due to ductile flexural failure. They served as a U-wrap to reinforce the other two beams along the top and bottom faces of their respective positive and negative moment zones. Triaxial fabric-reinforced beams were found to be more ductile than C.F.R.P sheet-reinforced ones.

El-Refaie et al. (2003) The beams were externally bonded with CFRP sheets for flexural reinforcement and were divided into two groups based on the configuration of the internal steel reinforcement. Each group included a single reference beam that was not reinforced. All enhanced beams exhibited reduced ductility compared to the unreinforced control beams. It was observed that there was a maximum number of CFRP layers that could be applied before the beam's capacity began to level off. Another aspect of the study focused on whether extending the CFRP sheet to cover the entire hogging or sagging zones could alleviate the issue, as the peeling of the CFRP sheets was identified as the primary cause of failure in the tested beams. [10]

Ashour et al. (2004), R.C.C. continuous beams with various configurations of internal steel bars and outside CFRP laminates were used. With the same amount of internal steel reinforcement and identical geometrical specifications, three sets of test specimens were created. One control beam that wasn't reinforced and was intended to fail in flexure was added to each group. The concrete cover's link to the composite laminate failed due to peeling, laminate separation, and laminate rupture, three failure modes that were observed. Compared to the matched reference beam, each strengthened beam's ductility was decreased. There were also offered simpler approaches for calculating the interface shear stresses between the concrete material and the adhesive as well Concerning the flexural load capacity, the research focused on examining. They found, much like in earlier experiments, that extending the even with C.F.R.P sheet covering the whole positive or negative moment zone, the C.F.R.P laminates still peeled.[6]

In 2007, Aiello et al. The behavior of continuous R.C.C. The study examined beams reinforced with C.F.R.P. sheets in either positive or negative moment regions, as well as R.C.C beams reinforced in both positive and negative moment regions. All beams were strengthened using a single layer of C.F.R.P. sheeting, excluding loading at the mid-span of the beams. The failure of the control beams was attributed to the delamination of the C.F.R.P. sheets and concrete crushing, while the reinforced beams failed due to the debonding of the C.F.R.P. sheets and concrete crushing.

Akbarzadeh et al. (2010) An experimental program was conducted to gain a deeper

understanding of the flexural behavior and moment redistribution of continuous reinforced high-strength concrete (RHSC) beams reinforced with CFRP and GFRP sheets. The test results indicated that increasing the number of CFRP sheet layers improved the material's ultimate strength but led to a reduction in ductility, moment redistribution, and ultimate strain, consistent with previous studies. Strengthening continuous beams with GFRP sheets was found to reduce the loss of ductility and moment redistribution, although it did not achieve a significant enhancement in ultimate strength. The moment enhancement ratio for the reinforced continuous beams was notably higher than the ultimate load capacity enhancement ratio observed for the same beam. Additionally, they developed an analytical moment-curvature and load capacity model, which was applied to the tested continuous beams in this study and other related research.

2.1 OBJECTIVE & SCOPE OF OUR WORK

The main objective of this study is to investigate the behavior of RCC continuous beams reinforced with externally bonded GFRP (Glass Fiber Reinforced Polymer) sheets. The experimental examination focuses on the flexural strength of rectangular beams, which are categorized into two series: S_1 and S_2. Each series has different longitudinal and transverse steel reinforcement ratios, while maintaining consistent geometrical measurements. The beams are subjected to load at two points until failure, aiming to evaluate the extent to which the strengthening improves their flexural capacity. Additionally, a finite element model is employed to analyze and understand the behavior of the reinforced beams.

3. EXPERIMENTAL STUDY

For the experimental investigation, 11 massive 2 Span continuous rectangular R.C.C beams were casted. The flexural-weak beams are all cast and extensively tested. The beams were utilised to generate the findings of the S1 and S2 series. According to Tables 3.5 and 3.6 for Series S1 and S2, the longitudinal and transverse steel reinforcement ratios changed for each series. The geometrical characteristics of the beams, along with the loading and support arrangements, were carefully considered in this study, are depicted in Figure 3.6. Each beam is the same size: 152 mm in width, 305 mm in depth, and 2300 mm in length.

In order to examine the impact of strengthening strategies, one beam from each series (S1 and S2) was designated as a control beam without any enhancement. The remaining beams in both series were reinforced by applying externally bonded G.F.R.P sheets. Experimental data on load, deflection, and failure mechanisms were recorded for each beam. The investigation focuses on analyzing the changes in load-carrying capacity and failure mechanisms of the

beams, considering the different strengthening approaches employed.

3.1 SPECIMEN CASTING

In the experiment, cement, fine aggregate, and coarse aggregate are used in the following proportions: 1: 1.67: 3.33. During the mixing step, concrete mixture is employed. The beams require 28 days to heal. A total of six concrete cube specimens were cast alongside each beam during the initial casting phase and subsequently cured. The Tables 3.5 and 3.6 display the average concrete compressive strength (fck) for each beam after 28 days. To determine the uniaxial compressive strength, tests were conducted on the concrete cubes, which were constructed with dimensions of 150 x 150 x 150 mm.

Table 3.1 Design Mix Proportions

Description	Cement	Sand (Fine Aggregate)	Coarse Aggregate	Water
Mix Proportion (by weight)	1	1.67	3.33	0.55
Quantities of materials (Kg/m^3)	368.42	533.98	1231.147	191.58

3.1.1 REINFORCEMENT DETAILING

The same configuration for flexure and shear reinforcement is arranged for the same sequence of continuous reinforced concrete beams.

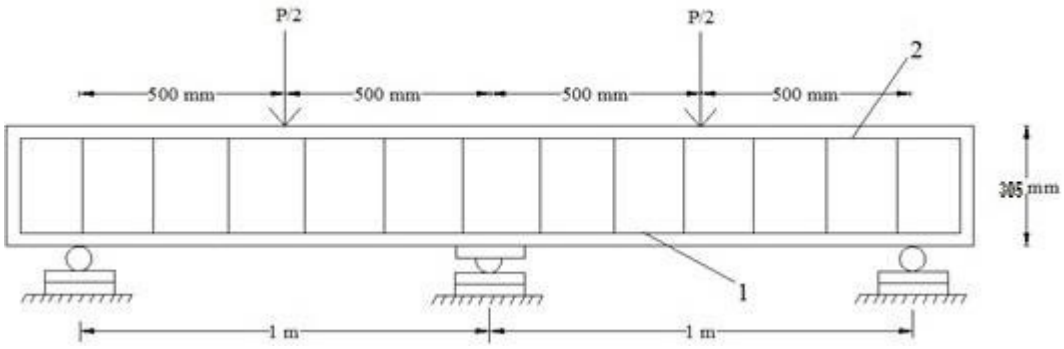

Figure 3.1 Detailing of reinforcement1, 2 – top and bottom steel reinforcement

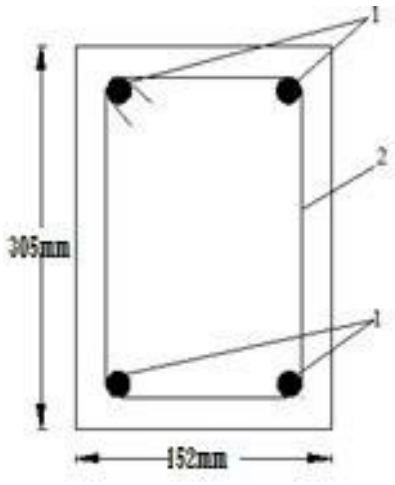

Figure 3.2 Cross section: 1 – Longitudinal rebar's, 2 – close stirrups

3.2 STRENGTHENING BEAMS

Before bonding the fiber, the concrete surface is roughened with coarse sandpaper and thoroughly cleaned with an air blower to remove any dirt or particles. The fiber textiles are then precisely cut to the required size, and the epoxy resin is prepared according to the manufacturer's instructions. Specifically, Araldite LY 556 and Hardener HY 951 are mixed in a 100:10 weight ratio in a plastic container. Once the epoxy glue is thoroughly mixed, it is applied to the prepared concrete surface. The GFRP sheet is then carefully placed over the epoxy coating, and a roller is used to press the resin through the fabric's roving, ensuring the removal of any trapped air bubbles. The process begins by roughening the concrete surface with coarse sandpaper, followed by cleaning with an air blower to eliminate dirt and particles. After cutting the fiber textiles to the correct size, the epoxy resin, made by mixing Araldite LY 556 and Hardener HY 951 in a 100:10 weight ratio, is applied to the concrete. The GFRP sheet is placed over the epoxy coating, and the resin is rolled through the fabric's roving to ensure proper impregnation and expel any trapped air bubbles.

Figure 3.4 Application of epoxy and hardener on the beam.

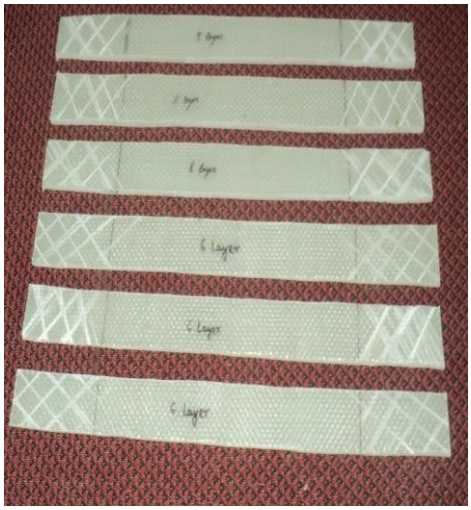

Figure 3.8 Specimens ready for tensile testing

Figure 3.10 Specimen failure after the tensile test

Table 3.3 Size of the specimens for tensile test

No. of layers	Length (cm)	Width (cm)	Thickness (cm)
2	15	2.3	0.1
4	15	2.3	0.25

6	15	2.3	0.3
8	15	2.3	0.45

3.2 DETERMINATION OF ULTIMATE LOAD, ULTIMATE STRESSAND YOUNG'S MODULUS (E)

To determine the ultimate stress, ultimate load, and Young's modulus, a unidirectional tensile test was conducted on specimens taken from the plates in both the longitudinal and transverse directions. Table 3.4 presents the measurements of these samples. The specimens were cut from the plates using either a diamond cutter or a hex saw, and they were subsequently polished using a polishing machine.

The INSTRON 1195 universal tensile test device was used to subject the specimens to failure at a predefined rate of extension in order to measure Young's modulus. Initially, the specimens were held by the upper jaw of the device, followed by the lower movable jaw. To ensure a secure grip and prevent slippage, the specimen was tightly held, with a 50 mm gauge length on each side. The strain was initially set to zero. Load and extension were digitally recorded using a load cell and an extensometer, respectively. This data was used to create a stress versus strain graph, with the Young's modulus determined from the initial slope of the graph. The final stress and load at the point of specimen failure were also determined. The average values for each layer of specimens are presented in Table 3.4.

Table 3.4 Result of the specimens

Thickness of the specime	**Ultimate stress**	**Ultimate Load (N)**	**Young's modulus(MPa)**
2 Layers	172.79	6200	6829.9
4 Layers	209.09	9200	7788.5
6 Layers	236.23	12900	7207.4
8 Layers	253.14	26200	7333.14

3.3 TESTING OF BEAMS

One by one, the fourteen beams are checked. They are all tested in the previously mentioned configuration. During the test, measurements of the dial gauge's deformation and the load's progressive increase are taken. The cracking load is the weight at which the first apparent crack appears. The weight is then kept on the beam until it ultimately breaks. The midpoint deflections of all beams, including those with and without GFRP, are measured and recorded as the load increases. The data presented in this chapter has been evaluated, and the results are discussed in the following chapter in order to reach a conclusion.

Table 3.5 Details of the Test Specimens for Series S1

Designationof Beams	**f_{cu} (MPa)**	**Main Longitudinal steel**		**Positive moment strengthening**		**Negative moment strengthening**	
		Top	*Bottom*	*No. of layers*	*Strengthened length(m)*	*No. of layers*	*Strengthened length(m)*
CB1	22.67	2-12 2-10*	2-8	-	-	-	-
SB1	23.3	2-12 2-10*	2-8	2	0.88m	6	0.88m
SB2	25.82	2-12 2-10*	2-8	4			
SB3	23.85	2-12 2-10*	2-8	2			
SB4	24.46	2-12 2-10*	2-8	4			
SB5	24.68	2-12 2-10*	2-8	4			

SB6	22.86	2-12 2-10*	2-8	4			

*provided at top tension zone

Table 3.6 Details of the Test Specimens for Series S2

Designation of Beams	**f_{cu} (MPa)**	**Main Longitudinal steel**		**Positive moment strengthening**		**Negative moment strengthening**	
		Top	*Bottom*	*No. of layers*	*Strengthened length(m)*	*No.of*	*Strengthened*
CB2	25.34	2-6, 2-10*	2-10	0	-	0	-
TB1	24.5	2-6, 2-10*	2-10	2	0.88m	6	0.88m
TB2	23.51	2-6, 2-10*	2-10	2			
TB3	25.61	2-6, 2-10*	2-10	4			

*provided at top tension zone

3.6.1. BEAM-1

CONTROL BEAM (C.B1)

CB1 failed in the conventional RC flexural mode due to the internal tensile steel reinforcement of the control beam. Significant flexural cracks developed at the mid-span and central support, extending deep into the compressive zones.

Figure 3.11 Experimental Setup of the C.B1

Figure 3.12 Flexural failure of C.B1

3.6.2 BEAM-2 CONTROL BEAM (C.B2)

The control beam, CB2 also failed in flexural failure as shown in Figure 3.13.

Figure 3.13 Control Beam, C.B2 after failure

3.6.3. BEAM-3 STRENGHENED BEAM 1 (SB1)

The beam was reinforced by applying six layers of FRP above the central support and two layers of FRP underneath the beam (each 150 mm wide) between two load locations, as depicted in Figure 3.14. As shown in Figure 3.15, the reinforced beam SB1 began to crack at a load of 110 KN and ultimately failed at 320 KN due to a debonding failure, where the FRP sheet detached from the concrete cover. The sudden rupture of the FRP sheet and the accompanying loud noise indicated a rapid release of energy and a complete loss of load capacity.

Figure 3.14 Experimental Setup of the Beam

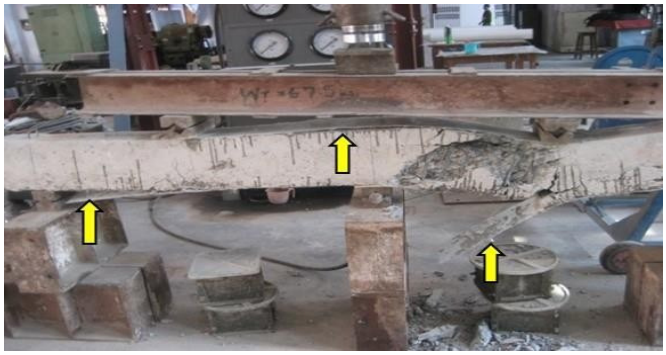

Figure 3.15 Deboning failure of FRP

Figure 3.16 Magnified view of the failure of the beam

3.6.4. BEAM-4

STRENGHENED BEAM 2 (S.B2)

A single layer of U-wrap was applied to the beam to prevent flexural failure. Tensile rupture occurred at the center of both the left and right sides of the FRP.

Figures 3.17 and 3.18 show how the beam failed in deboning with a concrete cover at low loads and developed a shear crack under the FRP covering as the load increased.

Figure 3.17 Tensile rupture of FRP at mid-section of right span at lower value

Figure 3.18 Ultimate failure of beam by deboning of FRP with concrete Cover

3.6.5. BEAM-5 : STRENGHENED BEAM 3 (S.B3)

To boost the load capacity, U-Jacketed double Layered GFRP was employed, as shown in Figure 3.19. By strengthening the beam with GFRP sheet, cracking of the RC beam may be delayed and flexural capacity increased. When the FRP sheet was deboned, the reinforced beam collapsed (Figure 3.20).

Figure 3.19 U-jacketed GFRP wrapped on the Beam SB3

Figure 3.20 Deboning failure of FRP

3.6.6 BEAM-6: STRENGHENED BEAM 5 (S.B4)

To prevent debonding, a full layer of U-wrap was applied over the two layers of FRP on the beam's soffit (150 mm wide), and a U-strip, 10 cm wide, was placed over the six layers of FRP above the central support. The failure mechanism was tensile rupture, and the U-strip failed to prevent the debonding of the upper FRP layer because it ruptured at higher load levels. However, the complete U-wrap successfully supported additional weight and prevented debonding.

Figure 3.22 Crack pattern after initial loading

Figure 3.23 Failure of the beam by tensile rupture

3.6.7 BEAM-7: STRENGHENED BEAM 5 (S.B5)

The same FRP configuration as SB4 was used, but to increase the strength of the beam, two layers of full U-wrap were used in lieu of one, and layers of U-strip with a width of 10 cm were put in place of one layer.

3.6.8 BEAM-8: STRENGHENED BEAM 6 (S.B6)

To avoid flexural failure, another two layers of FRP were put above the U-Jacketed double Layered GFRP in the flexural zone, but at half the width of the preceding two layers. Deboning failure occurred in this case rather than tensile rupture, as depicted. in Figure 3.27.

Figure 3.27 Deboning failure of Strengthened beam SB6

3.6.9 BEAM-9: T.B-1

As shown in Figure 3.37, the reinforced beam initially fractured at a load of 110 KN and subsequently failed due to debonding at 224 KN, causing the FRP sheet to detach from the concrete cover. The sudden rupture of the FRP sheet and the loud noise it generated signaled a rapid release of energy and a complete loss of load-carrying capacity. Strengthening the beam with a GFRP sheet can delay cracking in the RC beam and increase its flexural capacity.

Figure 3.36 Top FRP of Beam TB1 before Testing

Figure 3.37 FRP sheet separations without concrete

3.6.10 BEAM-10: TB2

A full double-layered U-wrap and six layers of FRP above the core support were used. 298 KN was the ultimate failure load.

Figure 3.38 Experimental set up and strengtheningpattern of TB2

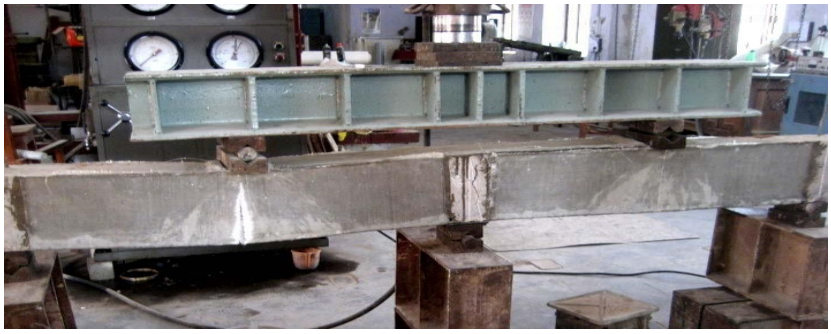

Figure 3.39 Failure of the beam by tensile rupture

3.6.11 BEAM-11:TB 3

To prevent flexural failure, two more layers of FRP were put above the U-Jacked double Layered GFRP at the flexural fracture zone, but at half the width of the previous two layers. The failure type was deboning failure rather than tensile rupture, as seen in Figure 3.41, and the failure load was 326 KN.

Figure 3.41 Failure of beam TB3

Figure 3.42 Shear crack in the left span

Figure 3.43 Failure mode of TB3

4. RESULTS AND DISCUSSIONS

This chapter provides an analysis of the experiment where concentrated loads were applied to the center of each span, and it presents the results in relation to the load-deflection curve and the observed failure mechanism. The chapter also provides explanations for the fracture patterns and collapse modes observed in each beam. When tested for final strength, it is found that the load-bearing capacity of the control beam is lower compared to the enhanced beam. Each set of beams, S1 and S2, included one beam evaluated as an unreinforced control, while the others were strengthened with various FRP sheet designs. As detailed in Tables 4.1 and 4.2, different types of beam failures were observed in both series, S1 and S2.

4.1 EXPERIMENTAL RESULTS

4.1.1 FAILURE MODES

4.1.1.1 CONTROL BEAM

Both control beams CB1 and CB2 experienced complete failure in terms of flexure. The failure initiation took place in the tension zone and then propagated to the compression zone, eventually resulting in flexural failure.

When the strain on the FRP (Fiber Reinforced Polymer) exceeds its designed rupture strain before the concrete strain reaches its maximum usable level, the FRP laminate is likely to fail. This failure of the GFRP (Glass Fiber Reinforced Polymer) laminate can cause debonding if the substrate cannot handle the forces exerted on the FRP. To prevent debonding of the GFRP laminate, it is crucial to keep the strain levels within the laminate under control.

Table 4.1 Experimental Results of the Tested Beams for Series S1

Designation of beams	**Failure Mode**	***Pu* (KN)**	$\frac{\text{Pu(strengthened beam)}}{\text{Pu(Control beam)}}$
CB1	Flexural failure	260	1
SB1	Debonding failure without concrete cover	320	1.23
SB2	Tensile rupture	325	1.25
SB3	Debonding failure without concrete cover	334	1.28
SB4	Tensile rupture	370	1.42
SB5	Tensile rupture	380	1.46
SB6	Debonding failure without concrete cover	415	1.59

Table 4.2 Experimental Results of the Tested Beams for Series S2

Designation of beams	**Failure Mode**	Pu **(KN)**	Pu(strengthened beam) / Pu(Control beam)
CB2	Flexural failure	200	1
TB1	Debonding failure	224	1.12
TB2	Tensile rupture	298	1.49
TB3	Debonding of FRP	326	1.68

4.2 LOAD DEFLECTION & LOAD CARRYING CAPACITY

The evaluation of the ultimate load-bearing capacity of G.F.R.P reinforced beams and control beams is conducted in this study. Deflection measurements are recorded at the midpoint of each beam's span or beneath the load point. The mid-span deflections of the reinforced beams are compared with those of the control beams. Notably, beams reinforced with GFRP sheets show improved flexural performance compared to control beams. The application of GFRP sheets reduces mid-span deflections, indicating increased stiffness. Reinforced beams demonstrate greater stiffness than control beams, and adding more GFRP layers generally further reduces mid-span deflection and enhances beam stiffness for the same applied load.

The use of GFRP sheets also affects fracture propagation within the beams. Tables 4.1 and 4.2 list the ultimate failure loads for all tested beams, including the ultimate load enhancement ratio, which compares the load capacity of externally reinforced beams to that of the control beams. The tables show that adding GFRP layers increases the ultimate load capacity, and incorporating an anchoring method could potentially enhance this load capacity even further.

4.3 DIAL GUAGE RESULTS OF TESTED BEAM SERIES S1

LOAD (KN)	Deflection(mm)																
	Midpoint to left span							Midpoint to right span									
	CB 1	SB 1	SB 2	SB 3	SB 4	SB 5	SB 6	CB 1	SB 1	SB 2	SB 3	SB 4	SB 5	SB 6	SB 7	SB 8	SB 9
0	0	0	0	0	0	0	0	0	0	0	0	0	0	0	0	0	0
50	0.5	2.0	0.3	0.9	0.5	1.0	0.5	0.5	2.3	0.5	0.9	0.6	1	0.6	1.6	0.5	0.8
100	1.7	2.8	1.0	1.3	1.1	1.5	0.9	1.8	3.0	1.0	1.3	1.2	1.5	1.0	2.0	1.0	1.3
150	2.5	3.3	1.9	1.9	1.6	2	1.3	3.0	3.7	1.8	1.9	1.7	2	1.4	2.4	1.5	1.5
200	3.8	3.9	2.9	2.4	2.3	2.5	1.6	4.5	4.5	2.5	2.5	2.5	2.5	1.7	3.0	2.1	2.0
250		5.7	5.0	3.0	2.5	3.5	1.8		6.0	4.4	4.8	3.1	3.5	1.9	3.6	2.9	
300				4.2	3.1	4.5	2.1				5.2	4.0	4.5	2.3		3.7	
350							2.6							2.8			

4.1.2.1 STRENGTHENED BEAM OF S1 SERIES

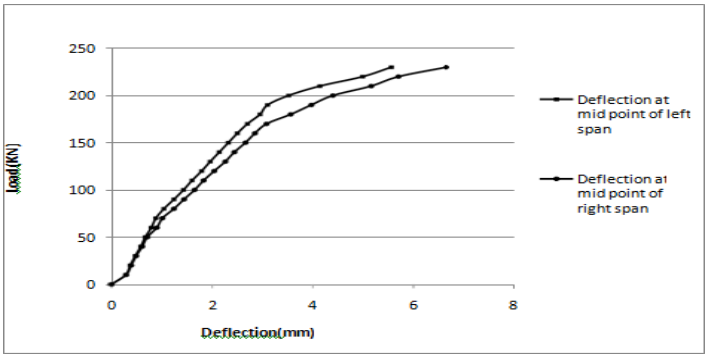

Figure 4.1 Load versus Deflection Curve for CB1

Due to its lack of reinforcement and low flexural performance, Beam 1 was assigned as the control beam (C.B1). The beam was subjected to static loading at two designated locations, and dial gauges were utilized to measure deflection at the midpoint of each span for each incremental load. Based on this data, a load vs. deflection curve was plotted to visualize the relationship between the applied load and the resulting deflection.

With a load of 70 KN, the first hairline fractures formed. When the force levels were increased subsequently, the fracture spread further. At 260 KN, the Beam C.B1 shattered totally in flexure.

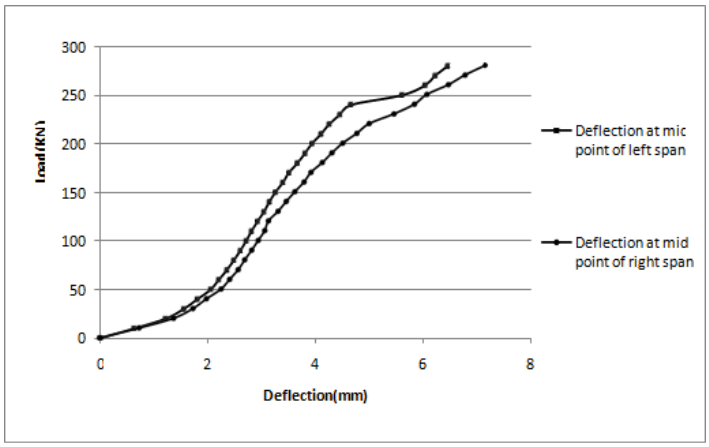

Figure 4.2 Load versus Deflection Curve for SB1

Beam-2, referred to as S.B1, was strengthened by applying G.F.R.P (Glass Fiber Reinforced Polymer) to the soffit (underside) of the beam, spanning from one support to another, as well as at the top section between the two designated load locations. Deflection values were recorded at the midpoint of each span, and a load versus deflection curve was plotted using this data. It was observed that the deflection values for S.B1 were lower compared to the control beam for the same applied load. The first hairline cracks appeared when the load reached 110 KN. As the force levels were subsequently increased, the fractures propagated more extensively. At lower loads, the G.F.R.P reinforcement without a concrete cover experienced debonding, where the G.F.R.P laminate detached from the concrete surface. Eventually, S.B1 failed when the concrete in the beam was crushed under an ultimate load of 320 KN.

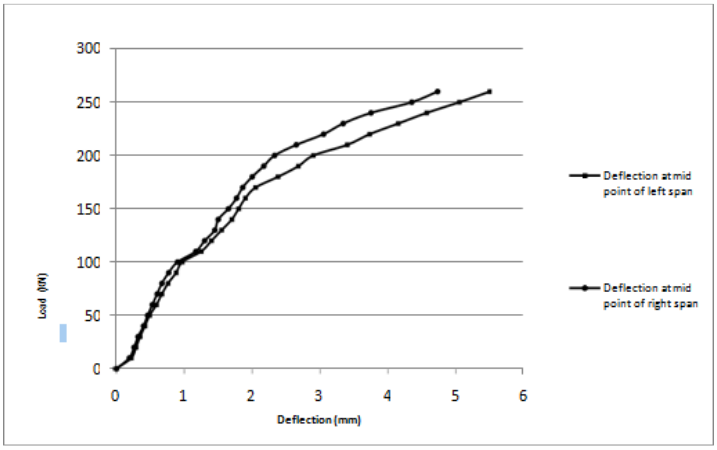

Figure 4.3 Load versus Deflection Curve for SB2

Beam-3, known as S.B2, was reinforced using a U-wrap configuration, which involved applying G.F.R.P (Glass Fiber Reinforced Polymer) reinforcement from one support to another

and between the two load points at the top section of the beam. The deflection values for S.B2 were found to be lower than those of the control beam for the same applied load. The presence of the G.F.R.P coating on S.B2 prevented the occurrence of early hairline fractures. However, as the loading values increased, fractures began to propagate beneath the G.F.R.P reinforcement. At lower loads, tensile rupture took place, followed by debonding of the G.F.R.P with a concrete cover as the load further increased. Ultimately, the beam collapsed in shear, experiencing failure at a force of 325 KN.

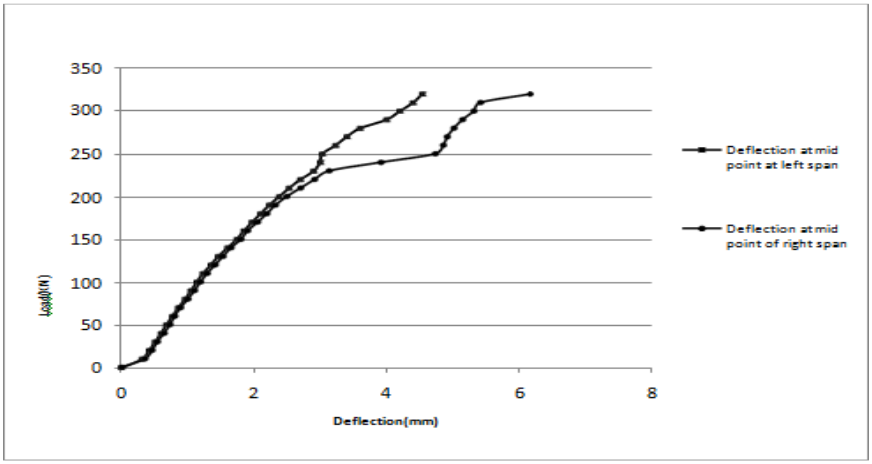

Figure 4.4 Load versus Deflection Curve for SB3

Beam-4, referred to as S.B3, was reinforced using U-wrap configuration, extending from one support to another. Additionally, extra layers of reinforcement were applied at the top section of the beam between the two stress points. However, despite the reinforcement, the beam ultimately failed due to debonding of the F.R.P (Fiber Reinforced Polymer) without a concrete cover.

Comparing deflection values for the same applied load, S.B3 exhibited significantly lower deflections compared to both the control beam and S.B1. The cracking load, where the first cracks appeared, was measured at 120 KN. Eventually, the beam failed at a load of 334 KN due to debonding of the F.R.P reinforcement without a concrete cover.

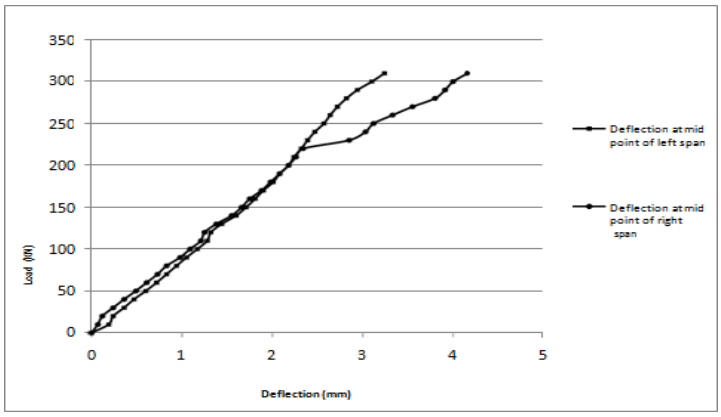

Figure 4.5 Load versus Deflection Curve for S.B4

Beam-5, designated as S.B4, underwent reinforcement with FRP (Fiber Reinforced Polymer) at the top section of the beam between the two load points, as well as a U-strip above it. Additionally, the beam was reinforced at the soffit, extending from one support to another. Tensile rupture occurred in the F.R.P without a concrete cover, and as the loading values increased, the crack beneath the G.F.R.P reinforcement expanded further. Eventually, the beam failed in flexure.

The failure load of S.B4 was recorded at 370 KN. Similar to previous cases, the deflection values for S.B4 were substantially lower than those of the control beam when subjected to the same load.

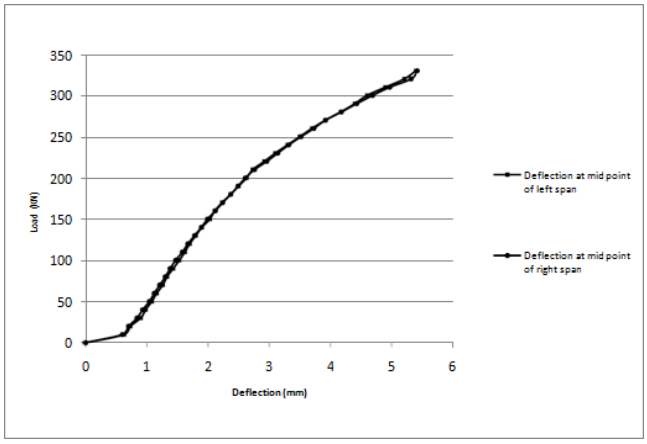

Figure 4.6 Load versus Deflection Curve for SB5

Beam-6, denoted as S.B5, was reinforced using F.R.P (Fiber Reinforced Polymer) at the soffit from one support to another, as well as above it in the form of U-wraps. Additionally, reinforcement was applied at the top section of the beam between the two load points and above

it in the form of U-strips. In comparison to previous cases, S.B5 had a higher number of F.R.P layers in the U-wrap and U-strip configurations.

Tensile failure began at lower loading levels for S.B5, and as the loading values increased, the crack beneath the G.F.R.P reinforcement continued to propagate until the beam ultimately collapsed in flexure.

Similar to the other reinforced beams, S.B5 exhibited lower deflection values compared to the control beam when subjected to the same load. The failure load of S.B5 was measured at 380 KN. Interestingly, the ultimate load of S.B5 was greater than that of S.B4, even though both beams had the same F.R.P wrapping pattern.

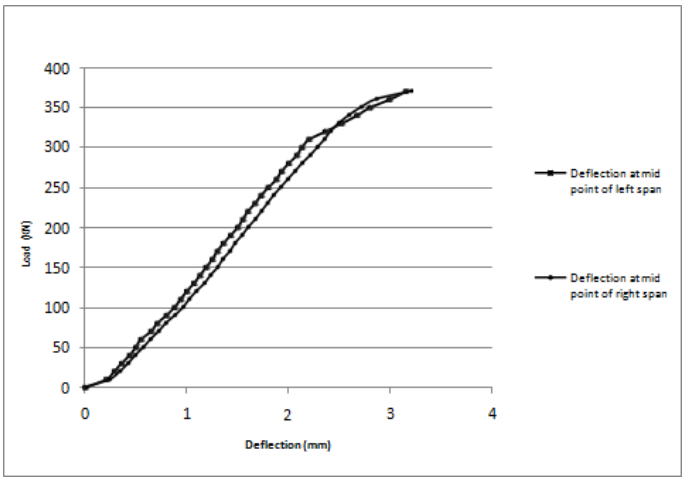

Figure 4.7 Load versus Deflection Curve for SB6

Beam-7, identified as S.B6, was strengthened using U-wrap F.R.P (Fiber Reinforced Polymer) reinforcement extending from one support to another, with an additional layer placed above it at half the width. Furthermore, reinforcement was applied between the two load points at the top section of the beam. During the loading process, the F.R.P reinforcement without a concrete cover experienced debonding. As the loading values increased, the crack beneath the G.F.R.P continued to widen until the beam eventually failed in flexure. Similar to the previously discussed reinforced beams, S.B6 exhibited significantly lower deflection values compared to the control beam when subjected to the same load. The failure load of S.B6 was recorded at 415 KN.

In Figure 4.11, the midpoint deflection values of each reinforced beam were separately compared to the control beam C.B1, and it was revealed that adding G.F.R.P to the beams increased their stiffness while somewhat decreasing their deflection values.

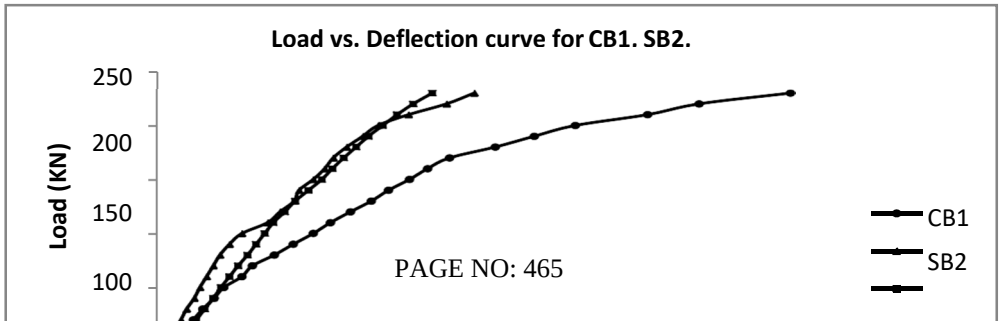

Figure 4.12 Load versus Deflection Curve for CB1, SB2, and SB3

In order to reinforce the beams, S.B3 was strengthened with two layers of U-wrap, while S.B2 had one layer added. Figure 4.12 illustrates a comparison of the mid-span deflections between the reinforced beams and the control beam. By reinforcing the beams and adding more G.F.R.P layers, the deflection values are reduced. This reduction in deflection indicates an improvement in beam stiffness, although the improvement is relatively small.

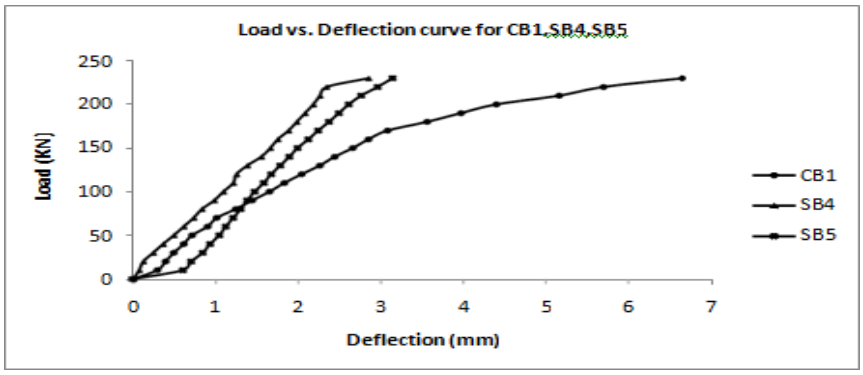

Figure 4.13 Load versus Deflection Curve for C.B1, S.B4, and S.B5

S.B4 was reinforced using one layer of U-wrap and U-strip, while S.B5 had two layers of U-wrap and two layers of U-strip added. Figure 4.13 illustrates a comparison of the mid-span deflections between these reinforced beams and the control beam.

In the case of S.B7, G.F.R.P reinforcement in the form of U-wrap was applied in two layers below the neutral axis and four layers above it. S.B8 further increased the number of G.F.R.P layers to three below the neutral axis and six above it. The midpoint deflections of S.B1 and S.B8 were compared to that of C.B1. The graphs depicted in the figure indicate that by adding more G.F.R.P layers, the stiffness of the beam can be increased.

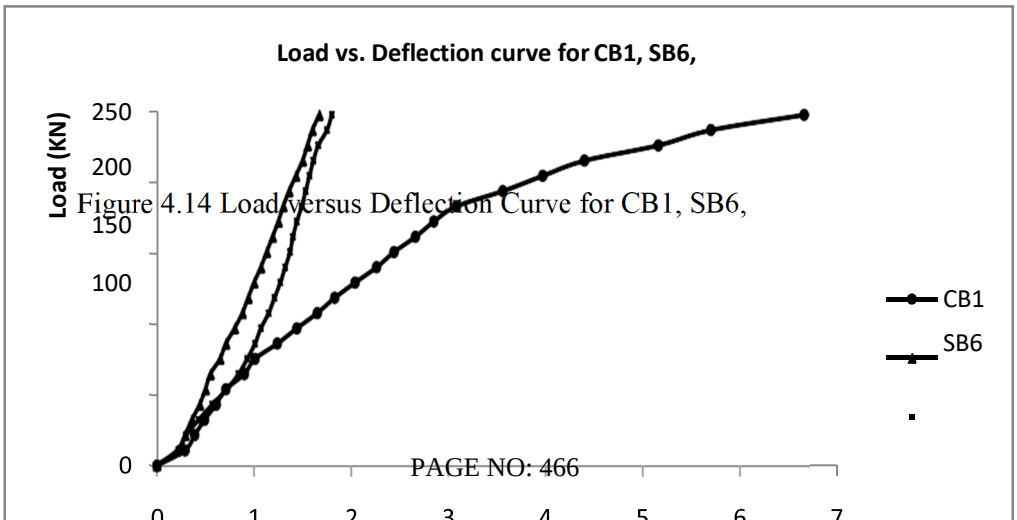

Figure 4.14 Load versus Deflection Curve for CB1, SB6,

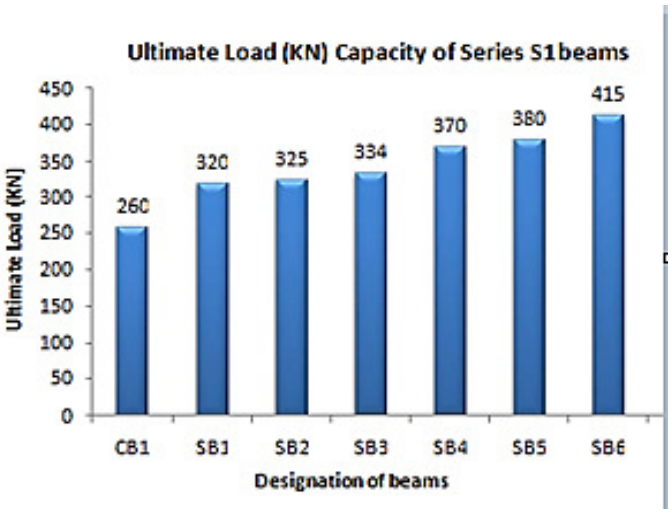

Figure 4.15 Ultimate Load Capacity of Series S1 beam

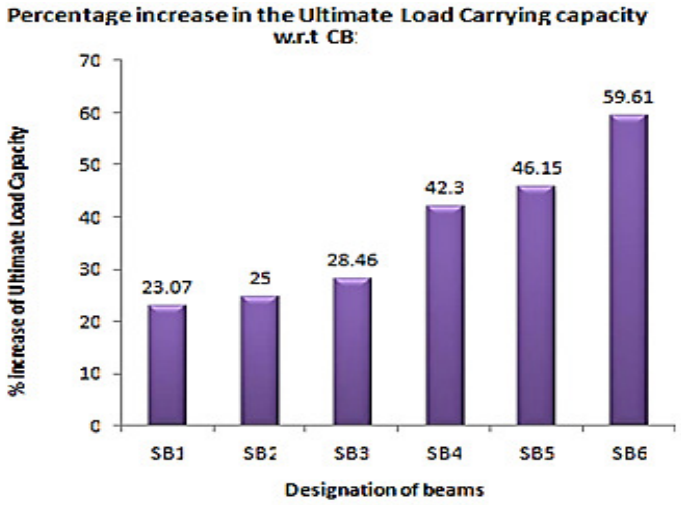

Figure 4.16 Percentage increase in the Ultimate Load Carrying capacity of beams of S1 w.r.t CB1

Figure 4.15 clearly illustrates that among all the reinforced beams in Series S1, SB6 exhibits the highest load capacity, while SB7 has the second-highest load capacity. On the other hand, Figure 4.17 provides a visual representation of the expected percentage improvement in load capacity for all the beams. From these figures, it can be concluded that the addition of GFRP to the beams can enhance their load capacity. Notably, SB6 beams show the largest percentage increase in load capacity among all the beams.

Table 4.4 Dial Gauge Results of the Tested Beams for series s2

4.1.2.2 STRENGTHENED BEAM OF S2 SERIES

LOAD (KN)	DEFLECTION(mm)							
	MIDPOINT TO LEFT SPAN				MIDPOINT TO RIGHT SPAN			
	CB 2	TB 1	TB 2	TB 3	CB 2	TB 1	TB 2	TB 3
0	0	0	0	0	0	0	0	0
50	1.2	1.2	0.9	1.1	1.2	1.2	1.0	1.1
100	1.9	1.8	1.8	1.5	2.0	2.0	1.9	1.5
150	3.7	3.2	2.5	2.2	3.8	3.3	2.5	2.1
200			3.6	3.0			3.1	2.8

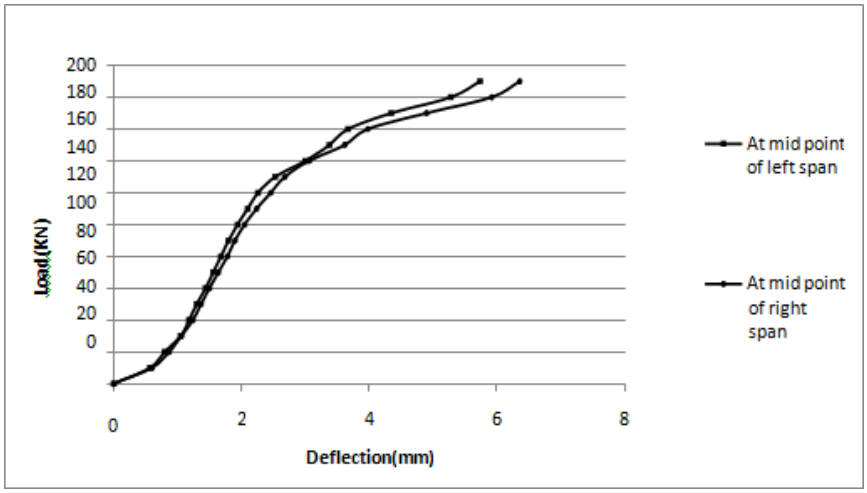

Figure 4.18 Load versus Deflection Curve for CB2

Beam 11, designated as C.B2 in set S.2, was tested under two-point static loading without any external reinforcement. Dial gauges measured the deflection at the midpoint of each span for each load increment. Using this data, a load versus deflection curve was created. Hairline cracks first appeared on the beam at a load of 110 KN, and the beam ultimately failed in flexure with a maximum load of 200 KN.

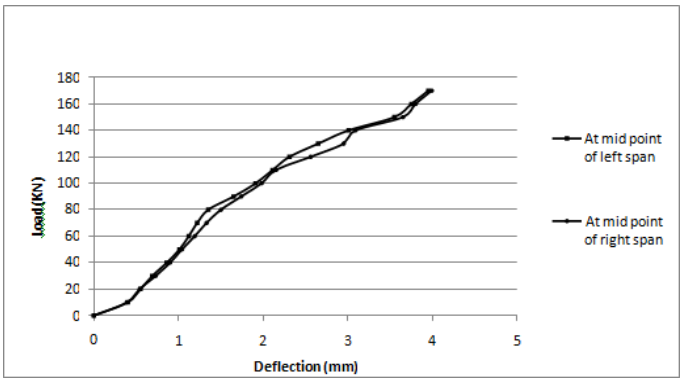

Figure 4.19 Load versus Deflection Curve for T.B1

Beam-12, also known as T.B1, underwent reinforcement from one support to another along the soffit and between the two top load locations. Deflection values were recorded at the midpoint of each span, and a load versus deflection curve was plotted. The deflection values of T.B1 were found to be lower than those of the control beam when subjected to the same load. However, at lower load values, debonding of the F.R.P (Fiber Reinforced Polymer) without a concrete cover occurred. Ultimately, T.B1 failed due to concrete crushing. The first hairline cracks appeared when the load reached 120 KN. As the loading values increased, the cracks propagated further, ultimately resulting in the beam snapping at an ultimate load of 224 KN.

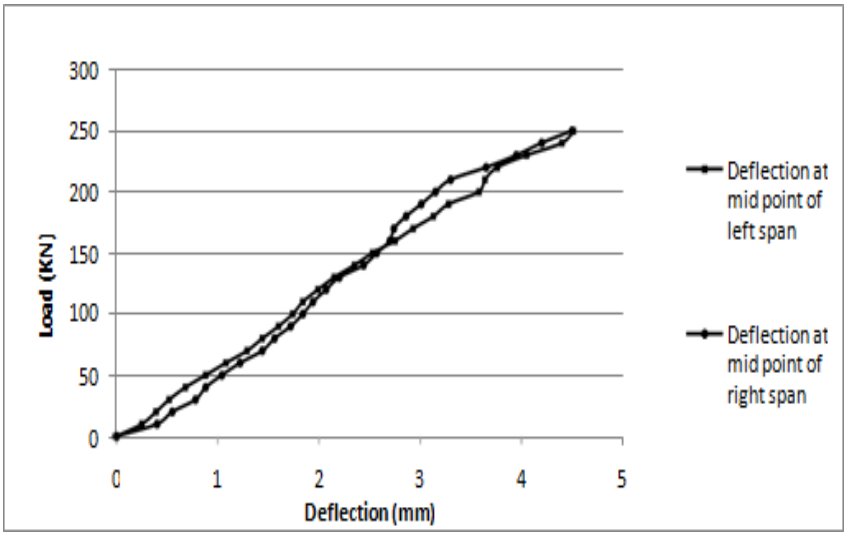

Figure 4.20 Load versus Deflection Curve for TB2

Beam-13, designated as T.B2, was strengthened with U-wrap reinforcement applied between the two load points at the top of the beam, extending from support to support. The number of reinforcement layers was notably increased. Under the same load, T.B2 exhibited lower deflection values compared to the control beam. The beam first failed due to tensile

rupture, followed by flexural collapse.

The onset of cracking occurred at a load of 210 KN, while the beam ultimately failed at a load of 298 KN.

Figure 4.21 Load versus Deflection Curve for T.B3

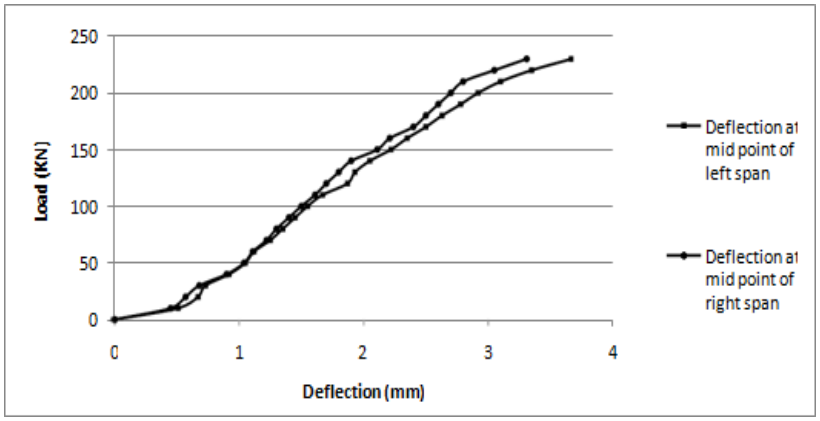

Beam-14, known as T.B3, experienced collapse due to the debonding of F.R.P (Fiber Reinforced Polymer) without a concrete cover, resulting in a shear crack. The deflection values of T.B3, at the same load value, are significantly smaller than those of both the control beam, C.B2, and the reinforced beam, T.B1. The failure load of T.B3 was measured at 326 KN.

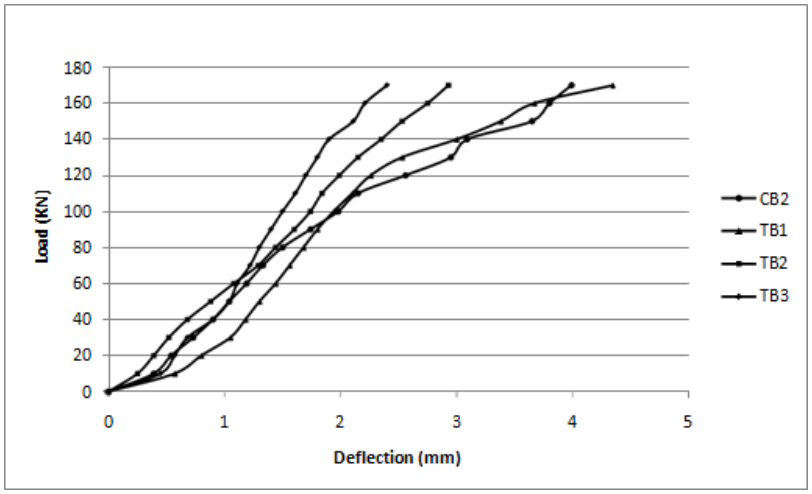

Figure 4.22 Load vs. Deflection Curve for all the Beams of S2

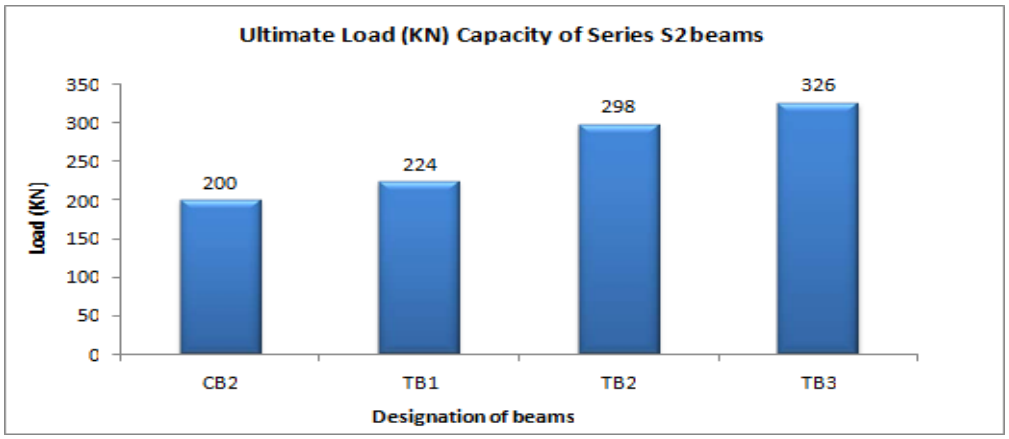

Figure 4.23 Ultimate Load (KN) Capacity of Series S2 beams

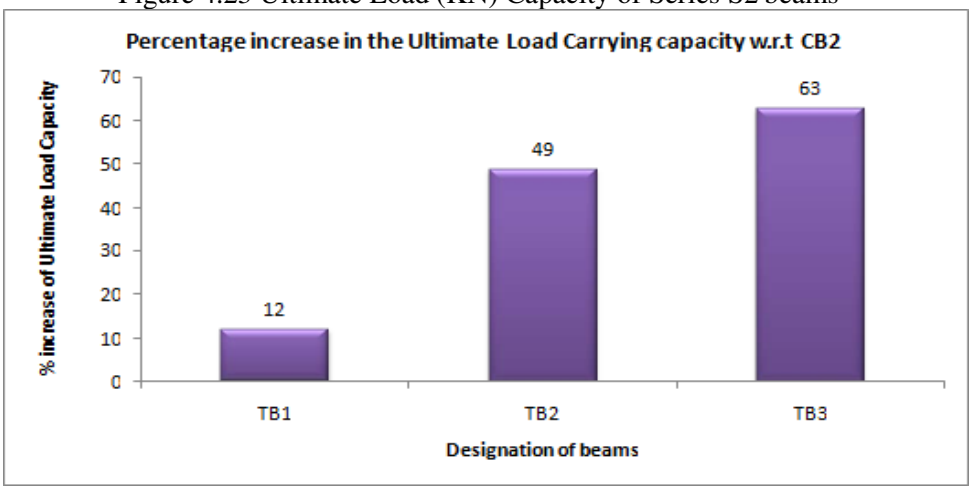

Figure 4.24 Percentage increase in the Ultimate Load Carryingcapacity of strengthened beams of S2 w.r.t C.B2

Figures 4.23 and 4.24 illustrate the load capacity and percentage increase of each reinforced beam in series S2. These figures clearly demonstrate that beam T.B3 exhibits the highest load capacity among all the reinforced beams. Additionally, T.B3 also demonstrates the greatest percentage increase in load-bearing capability compared to the other beams.

5. CONCLUSIONS

5.1 CONCLUSIONS

This research primarily focuses on investigating the flexural behavior of reinforced concrete rectangular beams using GFRP sheets. Fourteen RCC beams with various reinforcement details

were tested in two series, S1 and S2, to assess their flexural strength. Based on the test results and calculated strength levels, the following conclusions were drawn:

1. All reinforced beams demonstrated a higher ultimate load-bearing capacity compared to the control beam.
2. Cracking in the reinforced beams occurred at higher loads than in the control beams.
3. Beam S.B6, which incorporated two layers of U-wrap in the positive moment zone and two additional layers above the first two, exhibited a load-bearing capacity of 415 KN. This 59.61% increase in capacity underscores the effectiveness of using FRP to enhance the beam's load-carrying capacity in the flexural zone.
4. Beam T.B3 from Series S2, reinforced with two layers of U-wrap in the positive moment zone and two layers above the initial two, achieved a maximum ultimate load of 326 KN, representing a 63% increase in load-bearing capacity compared to similarly reinforced beams in the same series.
5. Using a steel bolt and plate system to secure the FRP sheet effectively prevents debonding failure.
6. Strengthening continuous beams by applying U-wraps of FRP sheets is an innovative and practical method to significantly increase their load-bearing capacity.

In summary, this research demonstrates the effectiveness of GFRP reinforcement in enhancing the flexural behavior and load-carrying capacity of RCC beams, with specific reinforcement configurations leading to substantial increases in strength. The use of steel bolt and plate systems and U-wraps of FRP sheets are identified as valuable techniques for improving the performance of reinforced beams.

REFERENCES

[1] ACI Committee 440, “Starte-of-the-art report on fiber reinforced plastic reinforcement for concrete structures”, Report ACI 440R-96, USA: *American Concrete Institute*, 1996.

[2] Aiello MA, Valente L, and Rizzo A, “Moment redistribution in continuousreinforced concrete beams strengthened with carbon fiber-reinforced polymer laminates”, *Mechanics of Composite Materials*, vol. 43, pp. 453-466, 2007.

[3] Aiello MA, and Ombres L, “Cracking and deformability analysis of reinforced concrete beams strengthened with externally bonded carbon fiber reinforced polymer sheet”, *ASCE Journal of Materials in Civil Engineering*, vol. 16, No. 5, pp.292-399,2004.

[4] Akbarzadeh H, and Maghsoudi AA, "Experimental and analytical investigation of reinforced high strength concrete continuous beams strengthened with fiber reinforced polymer", *Materials and Design*, vol. 31, pp. 1130-1147, 2010.

[5] Arduini M, and Nanni A, "Behavior of pre-cracked R. C. Beams strengthened with carbon FRP sheets", *ASCE Journal of Composites for Construction*, vol. 1, No. 2, pp. 63- 70, 1997.

[6] Ashour AF, El-Refaie SA, and Garrity SW, "Flexural strengthening of RC continuous beams using CFRP laminates", *Cement and Concrete Composites*, vol. 26, pp. 765- 775, 2003.

[7] Ceroni F, "Experimental performances of RC beams strengthened with FRP Materials", *Construction and Building Materials*, vol. 24, pp. 1547-1559,2010.

[8] Concrete Society, "Design guidance for strengthening concrete structures using fiber composite materials", Report No. 55, 71p, 2000.

[9] El-Refaie SA, Ashour AF, and Garrity SW, "CFRP strengthened continuous concrete beams", *Proceedings of the ICE - Structures and Buildings*, pp. 395 - 404, 2003.

[10] El-Refaie SA, Ashour AF, and Garrity SW, "Sagging strengthening of continuous reinforced concrete beams using carbon fiber sheets", *The 11th BCA Annual Conference on Higher Education and the Concrete Industry*, Manchester, UK, pp. 281– 292, 3–4 July 2001.

[11] El-Refaie SA, Ashour AF, and Garrity SW, "Strengthening of reinforced concrete continuous beams with CFRP composites", *The International Conference on Structural Engineering, Mechanics and Computation*, Cape Town, South Africa, 2–4. , pp.1591–1598, April 2001.

[12] Eshwar N, Nanni A, and Ibell TJ, "Performance of two anchor systems of externally bonded fiber-reinforced polymer laminates", *ACI Materials Journal*, vol. 105(1), pp. 72– 80, 2008.

[13] Garden HN, and Hollaway LC, "An experimental study of the influence of plate end anchorage of carbon fiber composite plates used to strengthen reinforced concrete beams", *Composite Structures*, vol. 42, pp. 175–188, 1998.

[14] Grace NF, Sayed GA, and Saleh KR, "Strengthening of continuous beams using fiber reinforced polymer laminates", *American Concrete Institute*, Farmington Hills, Mich, pp. 647-657, 2001.

[15] Grace NF, Wael R, and Sayed AA, "Innovative triaxailly braided ductile FRP fabric for strengthening structures", *7th International Symposium on Fiber Reinforce Polymer for Reinforced Concrete Structures*, ACI, Kansas City, MO, 2005.

[16] Grace NF, Abdel-Sayed G, Soliman AK, and Saleh KR, Strengthening of reinforced concrete beams using fiber reinforced polymer (FRP) laminates", *ACI Structural Journal*, vol. 96, No. 5, pp. 865-874, 1999.

[17] Grace NF, Soliman AK, Abdel-Sayed G, and Saleh KR, "Strengthening of continuous beams using fiber reinforced polymer laminates", *Proceedings of 4th International Symposium on Fiber Reinforced Polymer Reinforcements for Reinforced Concrete Structures*, SP-188, American Concrete Institute, Farmington Hills, Michigan, USA, pp.647-657, 1999.

[18] Jumaat MZ, and Alam MA, "Experimental and numerical analysis of end anchored steel plate and CFRP laminate flexural strengthened R. C. beams", *International Journal of Physical Sciences*, vol. 5, pp. 132-144, 2010.

[19] Jumaat MZ, Rahman MM, and Rahman MA, "Review on bonding techniques of CFRP in strengthening concrete structures", *International Journal of the Physical Sciences*, vol. 6(15), pp. 3567-3575, 4 August. 2011.

[20] K a d h i m , "Effect of CFRP Sheet Length on the Behavior of HSCContinuous Beam", *Journal of Thermoplastic composite materials*, Vol. 00, 2011.

[21] Khalifa A, Tumialan G, Nanni A, and Belarbi A, "Shear Strengthening of Continuous Reinforced Beams Using Externally Bonded Carbon Fiber Reinforced Polymer Sheets", *In: Fourth International Symposium on Fiber Reinforced PolymerReinforcement of Reinforced Concrete Structures,* Baltimore, MD, American Concrete Institute, pp. 995– 1008, November 1999.

[22] Leung CKY, and Cao Q, "Development of strain hardening permanent formwork for durable concrete structures", *Materials and Structures*, vol. 43(7), pp. 993–1007, 2009.

[23] Leung CKY, "Delamination failure in concrete beams retrofitted with a Bonded plate", Journal, 2001.

[24] Maghsoudi AA, and Bengar H, "Moment redistribution and ductility of RHSC continuous beams strengthened with CFRP", *Turkish Journal of Engineering and Environmental Sciences*, vol. 33, pp. 45-59, 2009.

[25] Niemitz CW, James R, and Berña SF, "Experimental behavior of carbon fiber- reinforced polymer (CFRP) sheets attached to concrete surfaces using CFRP anchors", *Journal of Composites for Construction*, vol. 12(2), pp. 185–194, 2010.